IOP Conference Series: Materials Science and Engineering

PAPER • OPEN ACCESS

Enhanced removal of Methyl Orange from aqueous solution by Chitosan-CaCl$_2$ beads

Enhanced removal of Methyl Orange from aqueous solution by Chitosan-CaCl₂ beads

V L Wong[1,*], S Y Tay[1] and S S Lim[2]

[1]School of Engineering and Physical Sciences, Heriot-Watt University Malaysia Campus, 62200 Putrajaya Wilayah Persekutuan, Malaysia.
[2]Department of Chemical and Environmental Engineering, University of Nottingham Malaysia Campus, Faculty of Engineering, Jalan Broga, Semenyih 43500, Malaysia

*Corresponding author : wong@hw.ac.uk

Abstract. Use of low-cost and environmental friendly sorbents has been studied as an ideal alternative to the current costly methods of removing textile dyes especially methyl orange from wastewater. In present study, the adsorption affinity of chitosan (CS)-CaCl₂ beads towards anionic acid dye, methyl orange was investigated by performing batch adsorption experiments. The surface morphology and elemental composition of CS-CaCl₂ beads were examined using Field Emission Scanning Electron Microscopy (FESEM) and Energy Dispersive X-ray Spectroscopy (EDX) respectively. The effects of initial dye concentration (20 to 100 mg/L), adsorbent dosage (0.05 g to 0.5 g), contact time (0 to 48 h), and agitation speed (0 to 300 rpm) were also studied to evaluate the efficacy of adsorption. Adsorption isotherm data of CS-CaCl₂ fitted well to Langmuir (R^2 = 0.9964) isotherm model, indicating that homogenous adsorbent surface. Kinetic studies showed that the sorption process followed pseudo-second-order rate that involves chemisorption process, indicating that the adsorption nature of dye on CS-CaCl₂ adsorbent. Based on the results, CS-CaCl₂ beads could be alternative cost effective adsorbents gaining prominence as a method for the removal of anionic acid dye from textile effluent. In conclusion, this study demonstrated a profound impact on improvement in water quality.

1. Introduction

In this 21st century, synthetic dyes are evidently utilized in many industries such as textile, food and pharmaceutical. With the increasing demand of textile products, environmental problems are emerging rapidly due to the large amounts of dye wastewater being released into the environment. From an annual production of 700 000 tonnes of dye, an approximate 5-15% of this amount originates from the textile industry [1, 2]. Many harmful chemicals come alongside the dyes in the effluents due to the processes associated in the textile industry such as bleaching. The use of natural dyes in mainstream textile industries are generally non-existent due to the discovery of cheaper and higher quality synthetic dyes [3]. The chemical additives coupled with the synthetic dyes pose a serious and harmful threat to the ecosystem if they are released into the environment without proper treatment. On top of that, the dyes are difficult to be removed from the effluent due to the nitrogen component and aromatic structure in dye functional groups [4, 5].

Physical, chemical and biochemical methodologies have been used for the effective removal of synthetic dyes. These methods include membrane separation, biological degradation, advanced oxidation process, and adsorption [6]. The synthetic dyes are complex in nature with recalcitrant and

stable structures, thus the process of degrading these dyes in the wastewater are commonly using conventional methods [1]. Recent developments have indicated that the adsorption method is favorable due to its wide availability, lower cost, as well as its recyclability [7]. The main disadvantage of using commercial adsorbents, such as biochar, minerals and polymer compounds, is the limiting active sites for the adsorption, thus decreasing their efficiency [7]. Therefore, much researches have been done on utilizing and improving the efficiency of dye removal of biosorbents. These biosorbents are more environmental friendly and effective in dye adsorption. Biosorption has been reported as an effective process for optimizing color removal from dye contaminated solutions. It is a physiochemical process that occurs naturally in certain biomass which allows it to passively concentrate and bind contaminants onto its cellular structure. Since 1980s, biosorption has been studied for sequestering of organic and inorganic species such as heavy metals, dyes and other organic pollutants by various microorganisms from wastewater.

Chitosan (CS) is a biodegradable amino-polymer obtained from deacetylation of chitin, which is naturally found on the shells of crustaceans like shrimps, prawns, crabs and fishes [8]. For instance, approximately half of a prawn's total body weight is termed as bio-waste, which implies that chitin is naturally very abundant [9]. Thus, chitosan can be a reliable and sustainable option for large scale treatments due to its availability. CS is effective in removing dyes due to the presence of its functional groups, amino and hydroxyl groups, allowing for increase in adsorption sites and therefore higher capacity and interactions of adsorption with dye molecules. The degree of deacetylation primarily determines the adsorption's effectiveness as a high degree of it presumably results in more amino groups, resulting in higher affinity to the dye molecules [10]. The molecular structure of the CS easily interact with alkyl, acetyl and carboxylic groups in most dyes on a molecular level through electrostatic attraction [8]. Generally, CS is able to dissolve in acidic solutions while being able to reform in basic conditions aid in the efficient removal of dyes [11]. Therefore, modifications need to be made onto the CS to improve its characteristics as an adsorbent. Improvements such as higher pH stability and increase in adsorption sites are beneficial to maximize the potential of CS as a commercialized bio-adsorbent.

In present paper, calcium chloride ($CaCl_2$) is selected as functionalizing agent to improve the number of available active sites which in turn might improve the efficiency of dye adsorption. The functionalization of polysaccharide-based CS using $CaCl_2$ has yet to be investigated for dye removal. Ca^{2+} ions are used to protonate the OH^- ions that are abundantly found in CS. This increases more active sites too specifically to have electrostatic interaction with methyl orange as anionic dye. Since methyl orange is an anionic dye, it can be predicted that the uptake efficiency can be increased with an increase in protonated active sites. Therefore, the functionalized CS beads would have better pH resistance and tensile strength after surface modification. In this case, the immobilization of Ca^{2+} ions onto CS beads was predicted to improve the adsorption capacity of beads towards anionic dyes, allowing better adsorption of the methyl orange dye. The extent of dye removal is dependent on the electrostatic attraction forces between the protonated chitosan beads with the SO_3^- group in anionic dyes such as methyl orange [13].

The ability of newly functionalized CS beads with $CaCl_2$ in decolorizing an anionic dye, methyl orange (MO) from the synthetic solution was compared and investigated in present studies. Systematic sets of experimental works were carried out to study the adsorption capacity of CS-$CaCl_2$, which turns out to be effectively governed by the $CaCl_2$ concentration, adsorbent dosage, contact time, agitation and initial concentrations. Subsequently, studies of sorption pattern, kinetics and mechanism onto functionalized CS beads were undertaken. By investigating these different parameters, the optimum standard of condition can be simulated at large to ensure this method of removal using functionalized CS beads with $CaCl_2$ can be successfully adopted as a large scale and commercially used treatment for anionic dye removal.

2. Materials and Methods

2.1. Biosorbent CS-CaCl$_2$ Preparation

CS powder with a deacetylation percentage of higher than 90% was purchased from Fulltime Asia Sdn. Bhd., Malaysia. CS solution was prepared by dissolving 4 g of CS powder into 196 g of 0.2 M acetic acid. The beads were formed by dropping the CS solution through a disposable plastic syringe with a 22 G needle tip, using syringe pump (AL-1000, Florida and NE-1000, Netherlands) operated at 8 mL/h into a bath containing 500 mL of 1 M NaOH, which was used to crosslink the CS droplets. Thus, CS beads were instantaneously formed in the alkaline medium under constant agitation at 200 rpm. A magnetic stirrer was used to stir the aqueous NaOH solution. The wet CS beads were filtered and thoroughly washed with distilled water to remove residual of NaOH. CS beads were then removed from the distilled water and chemically functionalized in a solution of CaCl$_2$ with concentration ranging from 0.005 M to 0.2 M for 24 h. The pH of each CaCl$_2$ solution was measured and recorded. The functionalized beads were oven-dried at 60°C until their weight was constant. The CS-CaCl$_2$ beads were then used as adsorbent for the sorption experiments subsequently.

2.2. Adsorbate Preparation

Methyl orange (MO), an anionic acid dye was selected as the key adsorbates in this study. Without further purification, MO stock solutions were prepared by dissolving accurately weighed dye sample in distilled water at a concentration of 1000 mg/L and other working solutions used in the experiment were obtained by dilution. Each concentration of working dye solution was determined using a UV/VIS spectrophotometer (HACH DR6000) operating in the visible range on absorbance mode. Absorbance values were recorded at the maximum absorbance wavelength (λ_{max} = 464 nm) and dye solution was initially calibrated for concentration in terms of absorbance units. A calibration curve with concentration of dye solution ranging from 10 to 100 mg/L was constructed.

2.3. Batch adsorption studies

Batch adsorption experiments were conducted by using constant mass of dried functionalized CS-CaCl$_2$ (0.1 g) in 60 mL of MO solution with concentration of 100 mg/L, unless otherwise stated. The mixture was stirred using an orbital shaker at 200 rpm and room temperature (21°C). After agitation for predetermined time intervals, the samples were withdrawn from the flasks and the dye concentration was determined spectrophotometrically.

Preliminary experiment was carried out by comparing the adsorption capacity (q_e) and MO uptake between the pure CS beads and functionalized CS beads with various concentration of CaCl$_2$ ranged from 0.005 M to 0.2 M. Next, the contact time needed for adsorption equilibrium was examined by adding 0.1 g of functionalized CS beads into 60 mL of 30 mg/L MO solution for 72 hrs. At fixed period of adsorption equilibrium, the effect of dosage of the 0.005 M CS-CaCl$_2$ dried beads for MO removal was investigated at different adsorbent doses ranging between 0.05 g and 0.5 g using 30 mg/L of MO solution. Apart from that, the effect of agitation speed for the biosorbent/sorbate adsorption system was studied at 0, 100, 200, and 300 rpm. On top of that, the effect of initial concentration on the adsorption behaviour of MO onto the CS-CaCl$_2$ dried beads was investigated in the range of 20 to 100 mg/L. The effect of each parameter was studied by fixing the values of other parameters. All the experiments were conducted in triplicate with a control and the average value were taken for analysis.

2.3.1. Equilibrium and Batch Kinetic Studies.

Equation 1 was used for determination of biosorption capacity of CS-CaCl$_2$ beads at different dye solutions at equilibrium state:

$$q_e = \frac{(Ci - Ce)V}{W} \tag{1}$$

where q_e is the adsorbed dye quantity per gram of CS-CaCl$_2$ beads at equilibrium (mg/g), C_i and C_e are initial and equilibrium MO concentrations in the solution (mg/L), V the solution volume (L) and W is the adsorbent dosage (g). The parameters in kinetics studies were identical to those of equilibrium tests. The aqueous samples were taken at preset time intervals, and the concentrations of the MO were similarly determined. The amount of dye adsorbed at different time intervals was calculated by using Equation (2):

$$q_t = \frac{(C_i - C_t)V}{W} \tag{2}$$

where q_t is the adsorbed dye quantity per gram of CS-CaCl$_2$ beads at any time (mg/g), C_i and C_t are initial and MO concentrations at time t in the solution (mg/L).

2.3.2. Langmuir and Freundlich Isotherm Model

In the present study, the Langmuir and Freundlich models were employed to study the equilibrium data in order to observe the sorption capacity of CS-CaCl$_2$ for MO dyes at different initial dye concentration.

Langmuir equation:

$$\frac{1}{q_e} = \frac{1}{q_{max}} + \left(\frac{1}{bq_{max}}\right)\left(\frac{1}{C_e}\right) \tag{3}$$

where q_e is the amount of MO adsorbed at equilibrium (mg/g), q_{max} is maximum sorption capacity corresponding to complete monolayer coverage (mg/g), and C_e the equilibrium MO concentrations in the solution (mg/L) and b is Langmuir constant related to the energy of biosorption (L/mg). A plot of $1/q_e$ versus $1/C_e$ for sorption of MO onto CS-CaCl$_2$ yields a straight curve of slope of $1/bq_{max}$ and intercept of $1/q_{max}$.

Freundlich equation:

$$\log q_e = \log K_f + \left(\frac{1}{n}\right)\log C_e \tag{4}$$

where K_f is Freundlich constant ((mg/g) (L/mg)$^{1/n}$) and 1/n is the Freundlich exponent (dimensionless). A plot of log qe versus log C_e for sorption of MO onto CS-CaCl$_2$ yields a straight curve of slope of $1/n$ and intercept of log K_f.

2.3.3. Kinetic Modelling Studies

The principle behind the adsorption kinetics involves the search for a best model that well represents the experimental data. Several kinetics models are available to understand the behaviour of the adsorbent and also to examine the controlling mechanism of the adsorption process and to test the experimental data. In the present investigation, the adsorption data at different initial dye concentration were analyzed using two simplest kinetics models, pseudo-first-order and pseudo-second-order kinetics models.

Pseudo-first-order rate equation:

$$\log(q_e - q_t) = log q_e - \frac{k_f}{2.303} t \tag{5}$$

Pseudo-second-order rate equation:

$$\frac{t}{q_t} = \frac{1}{k_s q_e^2} + \frac{1}{q_e} t \tag{6}$$

where q_t are the amount of MO adsorbed at time t, respectively (mg/g), k_f is the pseudo-first-order rate constant (1/h), k_s is the pseudo-second-order rate constant (g/mg h), t is the contact time (h) and q_e^2 is initial biosorption rate, h (mg/g h). For both kinetics models, the values of rate constant (k_f, k_s) and amount of MO adsorbed at equilibrium, q_e were determined from the slope and intercepts of the plot obtained by plotting log (q_e-q_t) versus time t (pseudo-first-order) and t/q_t versus time t (pseudo-second-order), respectively.

2.3.4. SEM-EDX Analyses

Morphological analysis was carried out using FESEM-EDX microscope (Quanta 400 F, USA) to identify the changes in the surfaces and structure of pure CS and functionalized CS-CaCl$_2$ beads before and after adsorption.

3. Results and Discussion

3.1. FESEM and EDX Analysis

The surface morphology of the prepared functionalized CS-CaCl$_2$ beads is illustrated with SEM images (Figure 1) and EDX analysis using software controlled digital scanning electron microscope.
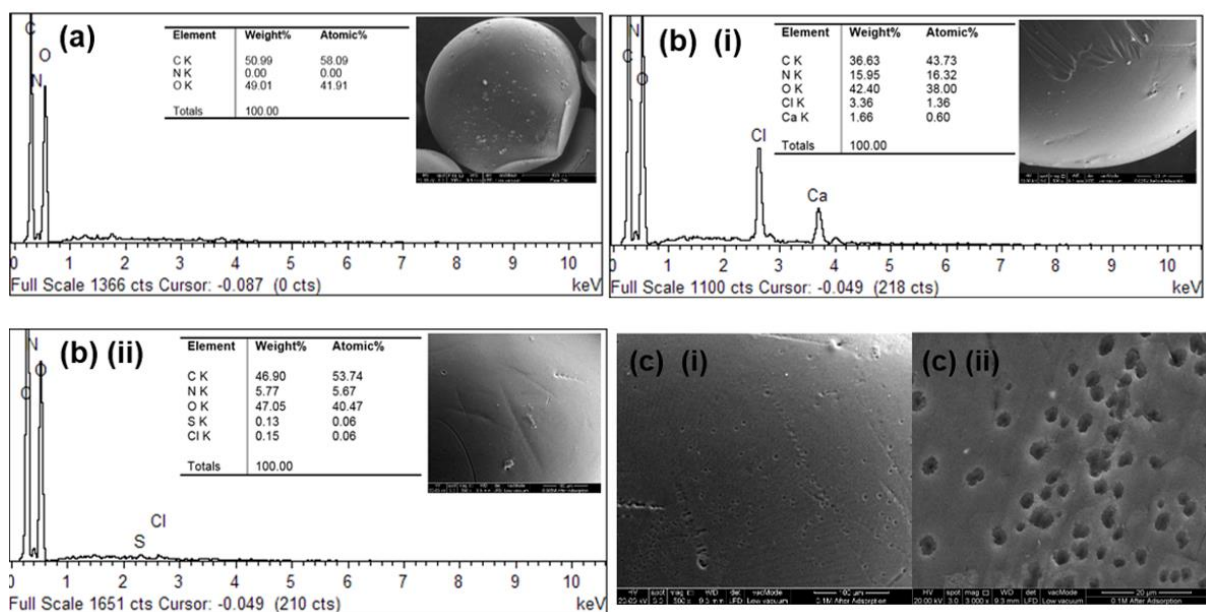

Figure 1. SEM+EDX analysis of (a) pure CS beads, (b) functionalized 0.005 M CS-CaCl$_2$ beads (i) before and (ii) after adsorption and (c) surface morphology of functionalized 0.1 M CS-CaCl$_2$ beads (i) before and (ii) after adsorption

As seen in Figure 1, the EDX spectrum of CS beads indicated the presence of C, N, and O but did not show the characteristic signal of Ca and Cl elements on the surface of pure CS beads. Before MO adsorption, the EDX spectrum was recorded for functionalized CS loaded with Ca and Cl ions, which give the characteristic peak for Ca and Cl at 3.69 keV and 2.64 keV, respectively. This confirms the binding of the Ca and Cl ions onto the surface of CS beads after functionalization. The characteristic signal of Ca and Cl ions has been significantly reduced for functionalized CS after MO adsorption. This could be explained by the formation of dye ion pairs and ion-pair associates between the protonated chitosan beads with the SO_3^- group in anionic dyes. Thus, the spectra intensity of Ca element is omitted when the immobilized Ca ions showing electrostatic interaction with dye ions in the collected EDX spectroscopy image (Figure 1(b) (ii)). As seen in Figure 1(c), the smooth intact surface of functionalized CS beads become more porous when the functionalized solution become more acidic as $CaCl_2$ concentration increases. At low pH, the acidic solution may attack the surface layer of biosorbents which induce pore formation, thus affecting the absorptivity of $CS-CaCl_2$ beads.

3.2. Selection of Potential Biosorbent

The adsorption capacity of $CS-CaCl_2$ and pure CS beads are compared in Figure 2. Figure 2 reveals that $CS-CaCl_2$ beads possessed higher sorption capacity (6.59 mg/g - 13.86 mg/g) in comparison with pure CS beads (3.97 mg/g). This sorption capacity of 0.005M $CS-CaCl_2$ beads was almost four times higher than pure CS-beads under identical sorption conditions. $CS-CaCl_2$ beads adsorbed anionic acid dye more effectively, while pure CS beads showed lower affinity towards the dye. The protonated Ca^{2+} ions on $CS-CaCl_2$ beads induce a higher number of active sites readily available for anionic MO dye. Furthermore, the higher affinity of $CS-CaCl_2$ beads for MO acid dye could be essentially explained by the changes in the permeability and surface charges on CS beads after surface functionalization. Consequently, the presence of Ca^{2+} ions on CS beads was proven to allow them to absorb higher amount of negatively charged dye molecules ($R-SO_3^-$).
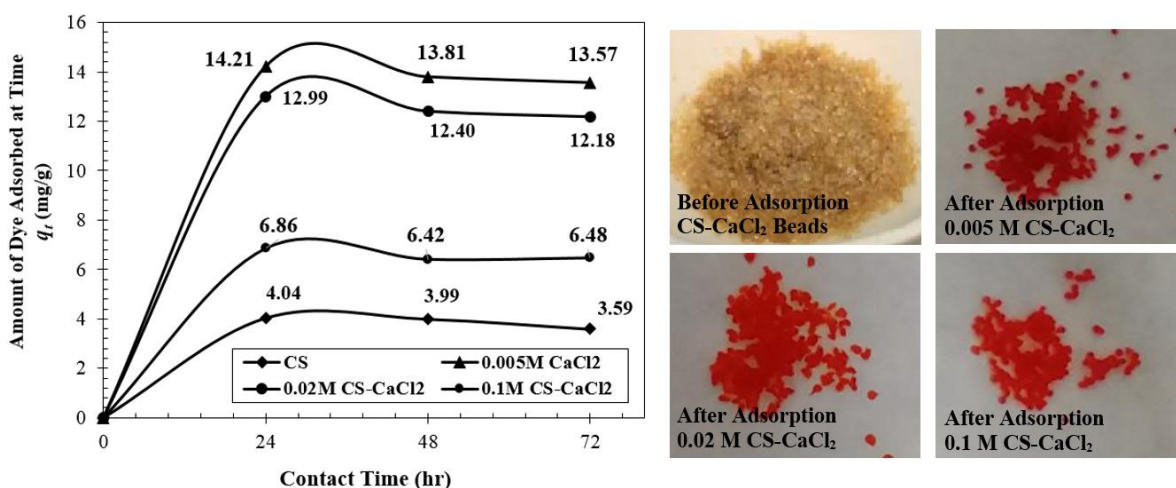

Figure 2. Adsorption capacity of CS and $CS-CaCl_2$ on removal of MO after 72 h. (V: 60 mL; Ci: 30 mg/L; W: 0.1 g; T: 21 °C; U: 200 rpm)

3.3. Effect of CaCl₂ Concentration

Figure 3 reveals that the CS beads functionalized with 0.005 M $CaCl_2$ showed the greatest adsorption capacity of MO. The pH of the differing $CaCl_2$ solutions also differs, with a lower $CaCl_2$ concentration giving a higher pH value and vice versa. Thus, initial pH sturdily affected the speciation and the adsorption availability of Ca^{2+} ions onto the surface of CS beads.
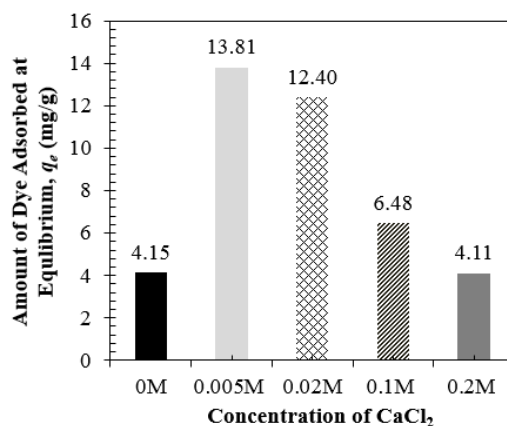
Figure 3. Adsorption capacity of CS-CaCl$_2$ on removal of MO at different functionalized concentration of CaCl$_2$ after 72 h (V: 60 mL; Ci: 30 mg/L; W: 0.1 g; T: 21 °C; U: 200 rpm)

CS has three reactive functional groups, such as an amino (-NH$_2$) group, primary and secondary hydroxyl (OH-) groups. The isoelectric point (pI) of CS, is defined as the specific pH where the CS has no net charge and is of neutral state [14]. If the pH has the same value as the pI, the CS will have net zero electrostatic charge. When pI > pH, the CS beads will tend to have a net positive charge and is more cationic in behaviour. When pI < pH, the CS beads will tend to have a net negative charge and is more anionic in behaviour [14]. With an increase in pH, deprotonation on the CS occurs [15]. The decrease in pH$_{H2O}$ was caused by the addition of CaCl$_2$ salt. Thus, at lower concentration of CaCl$_2$, the hydroxyl groups on the chitosan are prominently responsible for interaction with cation and positively charged group as pH increases. CS beads, with a more negatively charged surface, create more active sites for immobilizing Ca^{2+} ions on CS surface. Functionalization of the CS beads with Ca^{2+} ions becomes more effective at higher pH and it is evidently seen with the modification of CS beads in 0.005 M CaCl$_2$ solution (see Table A.1 in *Supplementary Data*). The CS beads functionalized with the 0.005 M CaCl$_2$ solution had the highest dye uptake of 73.78%. Ca^{2+} ions immobilized at concentration of 0.005 M allow effective electrostatic attraction to negatively charged MO dye molecules.

3.4. Effect of Contact Time

Adsorption time of MO acid dye removal was investigated from determination of absorbance value after adsorbed using functionalized 0.2 M CS-CaCl$_2$ dried beads. 0.1 g of 0.2 M CS-CaCl$_2$ dried beads was mixed with 30 ppm MO solution for various intervals of contact time (1 h, 2 h, 3 h, 4 h, 5 h, 24 h, and 48 h) at room temperature (21°C). As seen in Figure 4, the adsorption was rapid at the first 5 h as the adsorbent sites were vacant and solute concentration gradient was high. As contact time was further increased, the uptake rate started to stagnate, with a less steep gradient increase after equilibrium was reached. This might due to the unavailability of active binding sites which decreased with increasing of contact time [16]. Despite an increase in adsorption after the first 5 h, the minimum required time for optimum adsorption was achieved after 24 h.
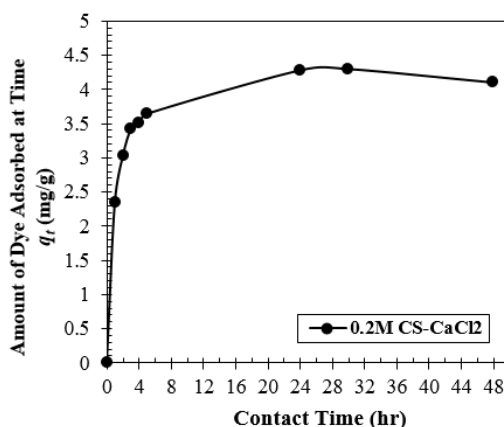
Figure 4. Adsorption capacity of CS-CaCl$_2$ beads functionalized with 0.2 M CaCl$_2$ on removal of MO. (V: 60 mL; Ci: 30 mg/L; W: 0.1 g; T: 21 °C; U: 200 rpm)

3.5. *Effect of Adsorbent Dosage*

The amount of dye adsorbed at equilibrium was the highest for the lowest dosage of the 0.005 M CS-CaCl$_2$ adsorbent at 0.05 g (14.1 mg/g) and lowest for the highest amount of adsorbent at 0.5 g (2.35 mg/g). Figure 5(b) reveals the highest dye uptake was recorded at 64.68 % by using 0.5 g dosage of CS-CaCl$_2$ dried beads. As the dye adsorption at equilibrium accounts for dye removed per gram of adsorbent dosage, certainly with a higher dosage, the dye adsorption at equilibrium value will be lower for a higher adsorbent dosage value (see Figure 5(a)). With a higher dosage of the CS-CaCl$_2$ beads, more MO dye ions can be adsorbed onto the active sites of beads, ultimately leading to a higher dye uptake. Similar observations were reported in previous studies [17]. Nevertheless, with the increasing of sorbent-to-solution ratio, the sorption capacity of available adsorbents was not fully utilized at higher dosage. Thus, addition of CS-CaCl$_2$ dried beads did not bring significant increase in adsorption tendency of adsorbate molecules. A further analysis of studying more than 0.5 g of beads could be considered for maximum dose beyond which no further beneficial effect was seen.
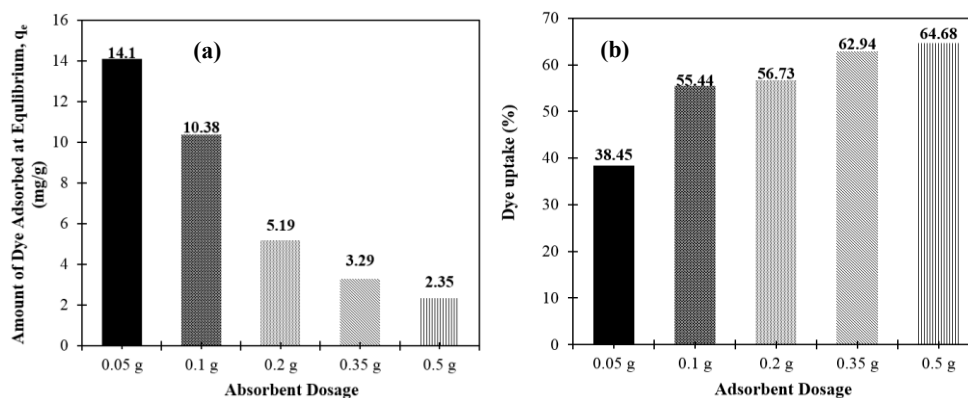

Figure 5. Effect of 0.005 M CS-CaCl$_2$ adsorbent dosage on (a) amount of MO adsorbed at equilibrium and (b) amount of MO uptake after 72 h (V: 60 mL; Ci: 30 mg/L; T: 21 °C; U: 200 rpm)

3.6. Effect of Agitation Speed

Figure 6 illustrates the sorption capacity of 0.005 M CS-CaCl$_2$ beads at different agitation speed. The most optimum agitation speed was at 200 rpm, as it yielded the highest dye sorption capacity of 9.88 mg/g.
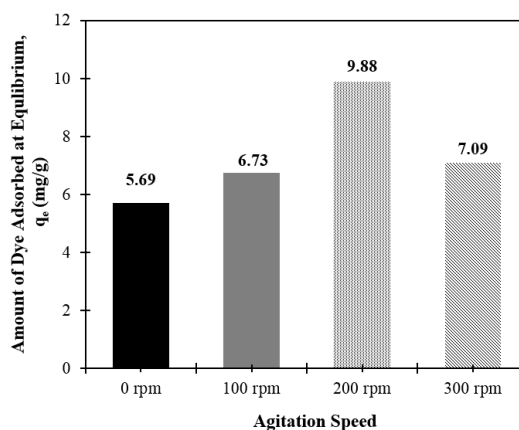

Figure 6. Effect of agitation on amount of MO adsorbed by CS-CaCl$_2$ beads functionalized with 0.005 M CaCl$_2$ after 72 h (V: 60 mL; Ci: 30 mg/L; W: 0.1 g; T: 21 °C)

Even though it may seem that with a higher agitation speed, it will result in a higher degree of collisions between the dye molecules and active sites, the dye adsorption at 300 rpm stagnates at only 7.09 mg/g. The adsorption value steadily increases with increasing speed from 0 rpm to 100 rpm and it finally reaches maximum adsorption capacity at 200 rpm. Therefore, it can be theorized that after a certain speed change, which in this case is any speed after 200 rpm, any agitation speed higher than that would decrease the adsorption uptake. The speed induced would be too fast to allow effective adsorption of the dyes onto the active sites beads to occur. An overly fast agitation speed would hinder and disturb the adsorption process, thus explaining the lower adsorption value obtained at 300 rpm. For speed increase from 0 rpm to 200 rpm, the steady increase in the adsorption levels is due to the enhanced bulk diffusion of the MO dye molecules. In this case, the higher the agitation speed, the thickness of boundary layer surrounding the chitosan-CaCl$_2$ adsorbent decrease, therefore resulting in an accelerated dye adsorption process [18]. This implies that there is an optimum agitation speed for successful dye removal.

3.7. Effect of Initial MO Dye Concentrations

Figure 7 shows the q_e value and dye uptake for MO respectively, with 90 ppm having the highest recorded q_e value at 6.99 and 30 ppm having highest dye uptake at 62.94 %. The trend for the q_e values gradually increases from 10 ppm to 90 ppm, confirming that with an increase in the initial dye concentration, mass transfer is now more likely to occur due to the increase in dye molecules [19]. The increase in mass transfer would ultimately result in an increase with adsorption of the dye molecules onto the 0.005 M CS-CaCl$_2$ dried beads. As for the dye uptake results, it increases from 10 ppm to 30 ppm, achieving peak dye uptake at initial concentration of 30 ppm, however it decreases once dye concentration increases from 50 ppm to 90 ppm. Aligning with the q_e results obtained, it can be concluded that the sorption capacity will be higher with an increase in the initial dye concentration, but the capacity plateaus decreases once the active sites on the CS-CaCl$_2$ beads are saturated [20]. This indicates that the sorption site of adsorbents has reached saturation for the higher amount of MO dye molecules to be absorbed at 50 ppm and 90 ppm.
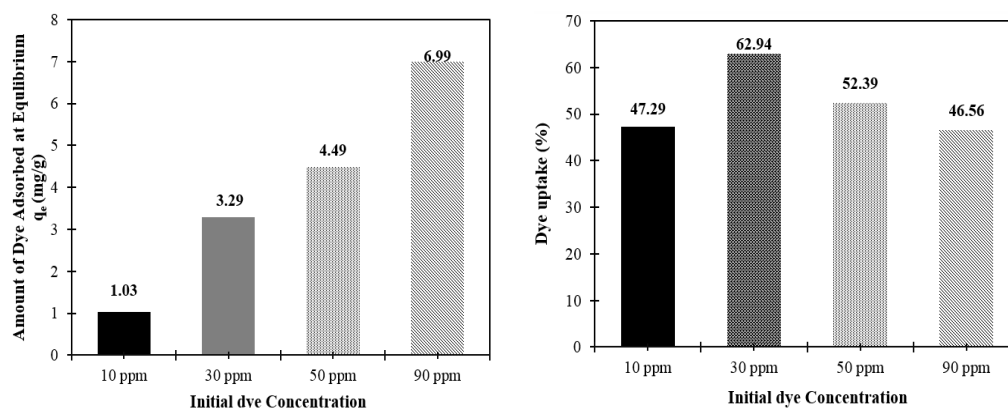
Figure 7. Effect of initial dye concentration on (a) amount of MO adsorbed at equilibrium and (b) its dye uptake of MO after 72 h (V: 60 mL; Ci: 30 mg/L; W: 0.35 g; T: 21 °C)

3.8. Biosorption Isotherm

Langmuir and Freundlich isotherms parameters for the adsorption of MO dyes studied onto CS-CaCl$_2$ beads are displayed in Table 1. In present studies, as seen in Table 1, the sorption of MO by CS-CaCl$_2$ beads are well-conforms to both Langmuir and Freundlich isotherm model. However, Langmuir model was better fitted than Freundlich model and show strong positive correlations, indicating that homogeneous distribution of active sites on the CS-CaCl$_2$ beads' surface. Thus, the higher correlation coefficient values ($R^2 = 0.996$) strongly imply the MO dye adsorption closely follows Langmuir isotherm models under the present experimental conditions.

Table 1. Langmuir and Freundlich constants for MO adsorption using linear regressive analysis

Isotherm	Parameters		
Langmuir	b **(L/mg)**	q_{max} **(mg/g)**	R^2
	0.0024	44.8430	0.9964
Freundlich	K_f **(mg/g)(L/mg)$^{1/n}$**	**1/n**	R^2
	0.1465	0.8744	0.9859

3.9. Kinetic Modelling Studies

The constant of pseudo-first-order and pseudo-second order models were shown in Table 2. The highest regression value (R^2) confirmed that the sorption data are well presented by pseudo-second-order kinetics, indicating that the rate limiting step of the system under study may be chemisorption which involves valency forces through sharing or exchange of electron between adsorbent and adsorbate. The rate of ion exchange reaction occurring on the surface is responsible for the removal kinetics and that the kinetic order of this reaction is two with respect to the number of adsorption sites available for the exchange.

Table 2. Rate constant of kinetics models at various initial dye concentrations

Initial dye concentrations, C_i (ppm)	$q_{e\,(exp)}$ (mg/g)	Pseudo-first-order rate constants			Pseudo-second-order rate constants		
		k_f	$q_{e(cal)}$	R^2	k_s	$q_{e(cal)}$	R^2
		1/hr	mg/g		g/mg hr	mg/g	
10	1.02	0.03	0.67	0.4363	0.00	1.08	0.9997
30	3.29	0.10	2.97	0.9923	0.69	3.34	0.9999
50	4.49	0.02	1.23	0.1880	1.30	4.67	0.9999
90	6.99	0.03	1.92	0.2656	0.93	7.19	0.9999

Note: $q_{e\,(exp)}$ – Experimental q_e value; $q_{e\,(cal)}$ – Calculated q_e value

4. Conclusions

Functionalized CS-CaCl$_2$ dried beads appeared to be more effective than pure CS dried beads for the removal of MO dye from aqueous solution due to its higher sorption capacity. Additionally, 0.005 M CS-CaCl$_2$ dried beads showed the highest q$_e$ value (14.21 mg/g) and selectivity for the MO dyes. The MO dye uptake was increased from 38% to 65% with increasing in adsorbent dosage from 0.05 g to 0.5 g of 0.005 M CS-CaCl$_2$ dried beads. This is mainly due to greater availability of surface area of the biosorbents. Additionally, the agitation speed significantly affected the sorption efficiency of 0.005 M CS-CaCl$_2$ dried beads and showed the highest MO dye uptake at 200 rpm. The batch experiments also revealed the importance of initial dye concentration in the biosorption of MO dye. Maximum MO dye uptake (62.94%) was achieved at 30 mg/L initial dye concentration. The equilibrium data fit best with the Langmuir model. Modelling of kinetic results showed that the sorption process of MO by functionalized CS-CaCl$_2$ dried beads was best described by pseudo-second-order kinetic. The findings indicated that functionalized CS-CaCl$_2$ dried beads could be employed as an effective, ready availability, inexpensive adsorbent for the removal of dye and colour from water and wastewater, in particularly for the removal of MO. A successful biosorption process not only depends on dye uptake performance of the biomass, but also on the constant supply of the biomass for the process.

5. Supplementary Data

Table A.1 shows the pH values for the different concentration of tested CaCl$_2$ solution.

Table A.1. pH value of different molarities of CaCl$_2$ solution.

Molarity of CaCl$_2$ solution (M)	pH (at 25ºC)
0.005	6.43
0.02	6.02
0.1	5.54
0.2	4.93

Acknowledgments

References

[1]   Katheresan, V., Kansedo, J. & Lau, S. Y., 2018. Efficiency of various recent wastewater dye removal methods: A review. Journal of Environmental Chemical Engineering, pp. 4676-4697.

[2]   Yang, X. et al., 2018. One-step fabrication of chitosan-Fe(OH)$_3$ beads for efficient adsorption of anionic dyes. International Journal of Biological Macromolecules, Volume 117, pp. 30-41.

[3]   León, O. et al., 2018. Removal of anionic and cationic dyes with bioadsorbent oxidized chitosans. Carbohydrate Polymers, pp. 375-383.

[4]   Shajahan, A. et al., 2017. Comparative studies of chitosan and its nanoparticles for the adsorption efficiency of various dyes. International Journal of Biological Macromolecules, pp. 1449-1458.

[5]   Zhai, L. et al., 2018. Fabrication of chitosan microspheres for efficient adsorption of methyl orange. Chinese Journal of Chemical Engineering, pp. 657-666.

[6]   Zhao, J. et al., 2018. Chitosan adsorbent reinforced with citric acid modified β-cyclodextrin for highly efficient removal of dyes from reactive dyeing effluents. European Polymer Journal, pp. 212-218.

[7]   Jiang, Y. et al., 2018. Cross-linked chitosan/β-cyclodextrin composite for selective removal of methyl orange: Adsorption performance and mechanism. Carbohydrate Polymers, pp. 106-114.

[8]   Subramani, S. & Thinakaran, N., 2017. Isotherm, kinetic and thermodynamic studies on the adsorption behaviour of textile dyes onto chitosan. Process Safety and Environmental Protection, pp. 1-10.

[9]   Cahú, T. B. et al., 2012. Recovery of protein, chitin, carotenoids and glycosaminoglycans from Pacific. Process Biochemistry, pp. 570-577.

[10]   Vakili, M. et al., 2014. Application of chitosan and its derivatives as adsorbents for dye removal from water and wastewater : A review. Carbohydrate Polymers, pp. 115-130.

[11]   Mahmoodi, N. M., Salehi, R., Arami, M., & Bahrami, H. 2011. Dye removal from colored textile wastewater using chitosan in binary systems. Desalination, 267(1), 64-72.

[12]   Crini G., Badot P., 2008. Application of chitosan, a natural aminopolysaccharide, for dye removalfrom aqueous solutions by adsorption processes using batch studies: a review of recent literature.Polym Sci 33:399–447

[13]   Luk, C. J. et al., 2014. A Comprehensive Study on Adsorption Behaviour of Direct, Reactive and Acid Dyes on Crosslinked and Non-crosslinked Chitosan Beads. *Journal of Fiber Bioengineering and Informatics,* pp. 35-52.

[14]   Hristova, S. H. & Zhivkov, A. . M., 2019. Isoelectric point of free and adsorbed cytochrome c determined by various methods. Colloids and Surfaces B: Biointerfaces, Volume 174, pp. 87-94.

[15]   Motta, F., Melo, B. & Santana, M., 2016. Deprotonation and protonation of humic acids as a strategy for the technological development of pH-responsive nanoparticles with fungicidal potential. New Biotechnology, 33(6), pp. 773-780.

[16]   Maurya, R., Ghosh, T., Paliwal, C., Shrivastav, A., Chokshi, K., Pancha, I., Ghosh, A. and Mishra, S., 2014. Biosorption of methylene blue by de-oiled algal biomass: equilibrium, kinetics and artificial neural network modelling. PloS one, 9(10), p.e109545.

[17]   Pathania, D., Sharma, S. and Singh, P., 2017. Removal of methylene blue by adsorption onto activated carbon developed from Ficus carica bast. Arabian Journal of Chemistry, 10, pp.S1445-S1451.

[18]   Lai, K. C. et al., 2019. Ice-templated graphene oxide/chitosan aerogel as an effective adsorbent for sequestration of metanil yellow dye. Bioresource Technology, Volume 274, pp. 134-144.

[19]   Masilompane, T. M., Chaukura, N., Mishra, S. B. & Mishra, A. K., 2018. Chitosan-lignin-titania nanocomposites for the removal of brilliant black dye from aqueous solution. International Journal of Biological Macromolecules, Volume 120, pp. 1659-1666.

[20]   Szygula, A., Ruiz, M., Guibal, . E. & Sastre, A., 2008. Removal of an Anionic Reactive Dye by Chitosan and its Regeneration. Greece, s.n.